Chaotic scattering with localized losses: *S*-matrix zeros and reflection time difference for systems with broken time-reversal invariance

Mohammed Osman [1] and Yan V. Fyodorov [1,2]
[1]*Department of Mathematics, King's College London, London WC26 2LS, United Kingdom*
[2]*L. D. Landau Institute for Theoretical Physics, Semenova 1a, 142432 Chernogolovka, Russia*

(Received 7 May 2020; accepted 15 June 2020; published 6 July 2020)

Motivated by recent studies of the phenomenon of coherent perfect absorption, we develop the random matrix theory framework for understanding statistics of the zeros of the (subunitary) scattering matrices in the complex energy plane, as well as of the recently introduced reflection time difference (RTD). The latter plays the same role for *S*-matrix zeros as the Wigner time delay does for its poles. For systems with broken time-reversal invariance, we derive the *n*-point correlation functions of the zeros in a closed determinantal form, and we study various asymptotics and special cases of the associated kernel. The time-correlation function of the RTD is then evaluated and compared with numerical simulations. This allows us to identify a cubic tail in the distribution of RTD, which we conjecture to be a superuniversal characteristic valid for all symmetry classes. We also discuss two methods for possible extraction of *S*-matrix zeros from scattering data by harmonic inversion.

DOI: 10.1103/PhysRevE.102.012202

I. INTRODUCTION

Wave scattering in cavities with chaotic classical ray dynamics has been studied intensively over the last few decades [1–4]. The use of random matrix theory (RMT) has allowed for a statistical description of quantities derived directly from the $M \times M$, energy-dependent scattering matrix $S(E)$, where M is the number of scattering channels; for recent reviews, see [5–7]. In an ideal flux-conserving system $S(E)$ is unitary, but in practice unavoidable losses, e.g., due to imperfect conductivity of the cavity walls, or leaks in connecting microwave waveguides [8–15], make the experimentally observed scattering matrix subunitary. To that end, a considerable effort has been invested in generalizing the random-matrix-based approaches to chaotic wave scattering in the presence of some form of absorptive loss [16–24]. In recent years, the interest in absorptive scattering has been stimulated by a proposal to construct the so-called coherent perfect absorber (CPA), which can be looked at as a scattering system (e.g., a cavity) with a small amount of loss that completely absorbs a monochromatic wave incident at a particular frequency [25]. Applications for a CPA may include optical filters and switches or logic gates for use in optical computers. Recently, a CPA in a rectangular cavity with randomly positioned scatterers and absorption due to a single antenna has been realized experimentally [26], paving the way for the construction of CPAs based on disordered cavities. In another recent experiment, a CPA was realized with a two-port microwave graph system, both with and without time-reversal symmetry [27]. In the framework of chaotic scattering, a CPA state corresponds to an eigenstate of the S matrix with zero eigenvalue at a real energy. This fact naturally motivates rising interest in a more general question of characterizing S-matrix complex zeros, which has not been systematically studied for wave chaotic systems with absorption until very recently [28,29]. This is in sharp contrast with the statistics of S-matrix complex poles, known as resonances, whose exact density in the complex plane (and more delicate characteristics) for systems with chaotic scattering has been systematically studied in the framework of the random matrix approach [30–42] with some aspects amenable to experimental verification [43–51].

As is well known, an important quantity directly related to resonance poles in a scattering system is the so-called Wigner time delay, the energy derivative of the total phase shift [52,53], which in systems with chaotic scattering can be measured experimentally [54] and whose various generalizations recently attracted much attention [55]. In particular, it has been suggested that complex zeros of the scattering matrix can manifest themselves in a very analogous way via a quantity called the reflection time difference (RTD), which, in principle, may be measured experimentally [56]. Note that the problem of characterizing the statistics of Wigner time delays and related quantities in the RMT framework (and beyond) has been attracting considerable interest in the last 25 years [57–72]; for reviews, see [33] as well as the more recent Ref. [73]. It is therefore natural to ask similar questions about the statistics of the RTD in systems with chaotic scattering.

The goal of the present paper is to provide some information on fluctuations of RTD in the framework of the RMT approach. To this end, we mainly consider systems with broken time-reversal symmetry, where the properties of the complex S-matrix zeros can be very efficiently studied nonperturbatively (in particular, for any localized losses as well as any channel coupling) by adjusting the method suggested for S-matrix poles in [34]. This approach allows us to verify (and then exploit) that the S-matrix zeros for an absorptive system form asymptotically a determinantal process in the complex plane, as long as the effective dimension N of the Hilbert space describing the cavity Hamiltonian in an appropriate energy range is considered large: $N \gg 1$. The explicit form for the two-point function is then used to study the RTD correlation function along the lines suggested in [56], in full analogy with similar studies of the Wigner time delay [74].

To begin with, let us recall that one of the most natural ways of incorporating localized losses into the RMT description is to associate them with additional (or "hidden") scattering channels. When those channels are numerous and weak, one can model in this way spatially uniform absorption, the idea possibly going back to [16]; cf. the discussion after Eq. (12) in the text below. For the nonperturbative localized setting, the corresponding construction has been proposed recently in [29] in a form closest to our needs. To this end, consider a closed cavity whose internal chaotic wave dynamics is modeled by an $N \times N$ RMT Hamiltonian H_0, coupled to M scattering and L absorbing channels, the latter representing the sources of localized loss. The vectors of couplings to scattering/absorbing channels are collected in an $N \times M$ ($N \times L$) matrix W (A). We also define the associated $N \times N$ matrices $\Gamma_W = \pi W W^\dagger$ and $\Gamma_A = \pi A A^\dagger$, of the ranks M and L, respectively, and we further assume $M + L < N$. It is also convenient to assume that the columns of W and A are mutually orthogonal:

$$\sum_{n=1}^{N} W_{na}^* A_{nb} = 0, \ \forall a = 1, \dots, \ M\&b = 1, \dots, L \tag{1}$$

being in addition orthogonal within each of the channel groups:

$$\sum_{n=1}^{N} W_{na}^* W_{nc} = \gamma_a \delta_{ac}, \quad \sum_{n=1}^{N} A_{nb}^* A_{nd} = \rho_b \delta_{bd}. \tag{2}$$

The above assumptions lead to the diagonal form of the ensemble-averaged scattering matrix, which describes only the resonant scattering associated with the creation of long-lived intermediate states. The condition (2) can be easily lifted (see, e.g., Appendix in [24] for a recent discussion and further references).

The construction of the energy-dependent flux-conserving $(M + L) \times (M + L)$ scattering matrix $\mathcal{S}$ is done following the standard procedure frequently referred to as the "Heidelberg approach" and going back to the seminal work of Ref. [75]; see also [33]. Adapting it to the present situation, one gets the following block form, cf. [29]:

$$\mathcal{S} = \begin{pmatrix} 1_M - 2\pi i W^\dagger D^{-1} W & -2\pi i W^\dagger D^{-1} A \\ -2\pi i A^\dagger D^{-1} W & 1_L - 2\pi i A^\dagger D^{-1} A \end{pmatrix}, \tag{3}$$

where we denoted

$$D(E) = E 1_N - H_0 + i(\Gamma_W + \Gamma_A). \tag{4}$$

The upper left block $S(E) := 1_M - 2\pi i W^\dagger D^{-1} W$ describes the scattering between M "observable" channels, and it has the following alternative representation:

$$S(E) = \frac{1_N - iK_A}{1_N + iK_A}, \quad K_A = \pi W^\dagger \frac{1}{E - H_0 + i\Gamma_A} W. \tag{5}$$

Note that due to the presence of hidden/absorbing channels encapsulated via $\Gamma_A \neq 0$, the matrix $S(E)$ is subunitary reflecting the loss of flux injected through the observable channels, which escapes via the hidden channels, and as such is treated as irretrievably absorbed. A similar representation holds for the lower right block $S'(E)$ after the replacement $W \leftrightarrow A$ everywhere.

Since $S(E)$ is subunitary, the positions of its zeros in the complex energy plane are no longer conjugates of the corresponding poles, and thus in principle it can be located in both half-planes. From (5) one can easily deduce that the determinant of $S(E)$ has the following form:

$$\det S(E) = \frac{\det[E 1_N - H_0 + i(\Gamma_A - \Gamma_W)]}{\det[E 1_N - H_0 + i(\Gamma_W + \Gamma_A)]}, \tag{6}$$

from which it is clear that the zeros z_n of $S(E)$ in the complex energy plane are the complex eigenvalues of the non-Hermitian matrix $H_0 + i(\Gamma_W - \Gamma_A)$. Writing a similar expression for $\det S'(E)$ and taking their ratio, we arrive at the following complex number:

$$\frac{\det S(E)}{\det S'(E)} = \frac{\det[E 1_N - H_0 + i(\Gamma_A - \Gamma_W)]}{\det[E 1_N - H_0 + i(\Gamma_W - \Gamma_A)]} \tag{7}$$

$$= e^{2i\phi(E)}, \tag{8}$$

which is obviously unimodular for real values of the energy E.

Now we follow the proposal of [56] and define the reflection time difference (RTD) as the energy derivative of the phase $\phi(E)$:

$$\delta\mathcal{T}(E) := -i \frac{\partial}{\partial E} \ln \frac{\det S(E)}{\det S'(E)} \tag{9}$$

$$= \sum_{n=1}^{N} \frac{2\, \mathrm{Im} z_n}{(E - \mathrm{Re} z_n)^2 + (\mathrm{Im}\, z_n)^2}. \tag{10}$$

Such a definition of RTD is inspired by the Wigner time delay, which has the same form as 10 but with the zeros z_n replaced by the complex S-matrix poles located in the lower half-plane of complex energies. Those are simply complex eigenvalues of another non-Hermitian matrix $\mathcal{H}_{\text{eff}} := H_0 - i(\Gamma_W + \Gamma_A)$ and will be denoted $\mathcal{E}_n = E_n - i\Gamma_n/2$, with condition $\mathrm{Im}\mathcal{E}_n = -\Gamma_n < 0$ due to non-negativity of $\Gamma_W + \Gamma_A$. The main difference between the RTD $\delta\mathcal{T}(E)$ and the Wigner time delay is that the former can be negative whereas the Wigner time delay is always positive in the present model in view of $\Gamma_n > 0$. The term "reflection time difference" comes from the fact that the phase of $\det S(E)$ gives the delay (averaged over the scattering channels) in the propagation of a nearly monochromatic wave due to scattering, relative to a perfectly reflecting cavity. Hence the RTD is the difference in this delay between the first M channels, deemed observable, and the last L channels, deemed absorbing. Let us stress, however, that equivalently in any flux-conserving two-terminal system one can always simply subdivide channels into two groups, most naturally in a two-terminal scattering setup, via the left/right division. Then $S(E)$ and $S'(E)$ in such a system simply describe reflection blocks of the total S-matrix. Note that RMT-based statistics of entries and eigenvalues of the reflection blocks are interesting by themselves, and because they are related to Wigner time delays, they have been studied from various viewpoints, e.g., in [18,63,71,76,77].

II. STATISTICS OF *S*-MATRIX ZEROS FOR SYSTEMS WITH BROKEN TIME-REVERSAL INVARIANCE

We have thus seen that the zeros z_n of $S(E)$ in the present approach are merely the complex eigenvalues of the non-Hermitian $N \times N$ random matrix $H_0 + i(\Gamma_W - \Gamma_A)$. As the zeros are the main constituents of the RTD (10), we briefly analyze the statistics of those zeros in the complex plane for wave-chaotic systems with broken time-reversal invariance, when the matrix H_0 is taken from the Gaussian unitary ensemble (GUE). Note that systems of such type can be studied experimentally; see, e.g., [78] and references therein.

Since we have assumed the orthogonality both inside and between the two groups of channels [see (1) and (2)], by exploiting the unitary invariance of the GUE part we can easily check that the matrix $\Gamma := \Gamma_W - \Gamma_A$ of rank $M + L < N$ can be chosen to be diagonal: $\Gamma = \mathrm{diag}(\gamma_1, \dots, \gamma_M, -\rho_1, \dots, -\rho_L, 0, \dots, 0)$. In the lossless case $L = 0$, Γ is necessarily positive and all n-point correlation functions have been derived in [34] in the limit $N \gg \max(M, n)$. We show in the Appendix which modifications are necessary to adapt the method [34] to the lossy case $L > 0$, again with $M, L \ll N$. The end result is the following determinantal form for the asymptotic n-point correlation functions for the eigenvalues z_n in the whole complex energy plane:

$$\lim_{N\to\infty} \frac{1}{N^{2n}} R_n\left(x + \frac{z_1}{N\pi\nu(x)}, \dots, x + \frac{z_n}{N\pi\nu(x)}\right) = \det[K(z_i, z_j^*)]_{1\leqslant i,j\leqslant n}, \tag{11}$$

where $x \in (-2, 2)$, $\nu(x) = \frac{1}{2\pi}\sqrt{4 - x^2}$ is the semicircular density of real eigenvalues of the GUE matrix H_0, and the kernel is given explicitly by

$$K(z, w^*) = \sqrt{F(z)F(w^*)} \times \int_{-1}^{1} du\, e^{i(z-w^*)u} \prod_{a=1}^{M}(g_a + u) \prod_{b=1}^{L}(h_b - u), \tag{12}$$

where for $z = \mathrm{Re}z + i\,\mathrm{Im}z$ we have

$$F(z) = \int_{-\infty}^{\infty} \frac{dk}{2\pi} \frac{e^{-2ik\,\mathrm{Im}z}}{\prod_{a=1}^{M}(g_a - ik)\prod_{b=1}^{L}(h_b + ik)}, \tag{13}$$

$$g_a = \frac{1}{2\pi\nu(x)}\left(\gamma_a + \frac{1}{\gamma_a}\right), \quad h_b = \frac{1}{2\pi\nu(x)}\left(\rho_b + \frac{1}{\rho_b}\right). \tag{14}$$

Let us first check the simplest limit of very many equivalent weakly coupled absorbing channels, namely $L \to \infty$, $\rho_b \to 0$, in such a way that the product $L\rho_b$ remains a finite constant. Following [16], one expects that the absorption becomes spatially uniform across the sample, and that all zeros z_n will be uniformly shifted downward in the complex plane by the same amount. Indeed, introducing the notation $L\rho_b = \epsilon/[\pi\nu(x)]$, $\forall b = 1, \dots, L$ and assuming it remains constant as $L \to \infty$, we see that we can replace $h_b \approx \frac{L}{2\epsilon}$, and easily verify that the kernel in (12) reduces to the $L = 0$ case but with the shift $\mathrm{Im}z \to \mathrm{Im}z + \epsilon$, in full agreement with the uniform absorption picture.

A less trivial, representative case to be considered next is that of equivalent scattering channels $g_a = g$, $\forall a = 1, \dots, M$, as well of equivalent absorbing channels $h_b = g_0$, $\forall b = 1, \dots, L$, but both couplings are not considered to be weak. The interesting limiting case arises if we again assume the channels are abundant, so that both $M \to \infty$ and $L \to \infty$, but in such a way that the ratio $\frac{L}{M} = p$ with $0 \leqslant p \leqslant 1$ remaining constant (the case $p > 1$ follows by replacing $p \to \frac{1}{p}$ and $M \leftrightarrow L$ and $g \leftrightarrow h$). Note that this limit is performed after first taking the $N \to \infty$ limit with M, L finite. In such a limit, the integrals over variables u and $k_{1,2}$ can be readily evaluated by the Laplace (saddle-point) method. The calculation can be performed for general p, g, g_0, but the resulting expressions are relatively cumbersome; here we present explicit formulas only for the special case $p = 1$ and $g = g_0$ when they are more elegant. The ensuing asymptotic mean density of complex zeros is supported inside the domain,

$$\left\{(x, y) : -2 \leqslant x \leqslant 2, -\frac{M}{g^2 - 1} \leqslant y \leqslant \frac{M}{g^2 - 1}\right\}. \tag{15}$$

Note that since g depends on x as $g \sim 1/\nu(x)$, the width of the support along the imaginary axis decreases monotonically to zero at $x \to \pm 2$. Inside the support, the density is constant near the real axis and decays as y^{-2} when $y = O(M)$: defining $\widetilde{\rho}(x, y) := \frac{\rho(x,y)}{\nu(x)}$, we then have

$$\widetilde{\rho}(x, y) = \begin{cases} \frac{g^2}{2\pi M} & \text{if } y = O(1), \\ \frac{g^2}{4\pi M\widetilde{y}^2}\left(1 + \frac{1}{\sqrt{1+4g^2\widetilde{y}^2}}\right) & \text{if } y = M\widetilde{y}. \end{cases} \tag{16}$$

For the general parameters p, g, g_0, the support of the density in the complex plane is given for $-2 \leqslant x \leqslant 2$ by

$$-\frac{M}{2}\left(\frac{p}{g_0 - 1} - \frac{1}{g + 1}\right) \leqslant y \leqslant \frac{M}{2}\left(\frac{1}{g - 1} - \frac{p}{g_0 + 1}\right). \tag{17}$$

Figures 1(a) and 1(b) show the eigenvalues of five 4000×4000 matrices with $M = L = 100$ and $g = g_0 = 1.25$ and $g = 1.25$, $g_0 = 5.05$, respectively.

In particular, we see that if $p = 0$ then the zeros are all in the upper half-plane, separated from the real axis by the gap $\frac{M}{2(g+1)}$. Remembering that for $p = 0$ zeros are mirror images of poles, this result is simply the $L = 0$ case of [34]. The gap in the poles distribution is the well-known feature first derived in [31] and [57] in the related but slightly different limit $M = O(N)$. It has profound consequences for underlying dynamics, and it also has a semiclassic significance, being related to the classic escape time [79,80]. Moreover, one can see that all the *S*-matrix zeros will still be in the same half-plane as long as $|pg - g_0| > 1 + p$ (upper half-plane for $g_0 - pg > 1 + p$ and lower for $pg - g_0 > 1 + p$). An illustration of such a situation is given in Fig. 1(b).

When $|z_1 - z_2| = O(1/N)$, the kernel can be reduced after some algebraic manipulations to the Ginibre-like form

$$|K(z_1, z_2^*)| = \widetilde{\rho}(z)e^{-\frac{\pi}{2}\widetilde{\rho}(z)|z_1 - z_2|^2}, \tag{18}$$

where $z = \frac{z_1+z_2}{2}$, and $\widetilde{\rho}(z)$ is from (16). Such a kernel was found in the $L = 0$ case when $M \to \infty$ [34] and is conjectured to be the universal form of the kernel for strongly non-Hermitian matrices [39].

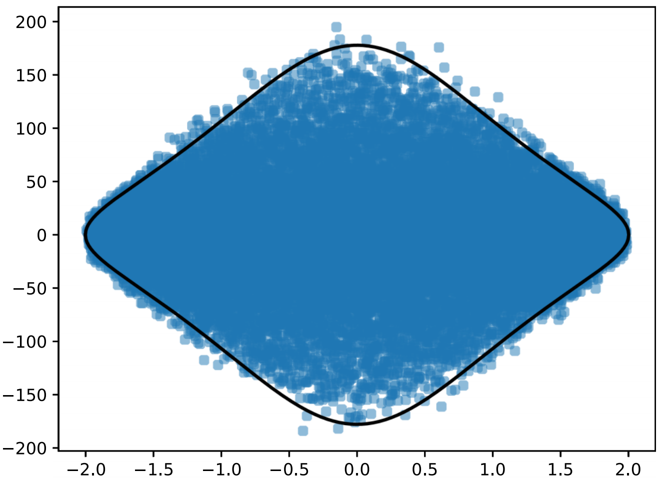

(a) $M = L = 100$ and $g = g_0 = 1.25$

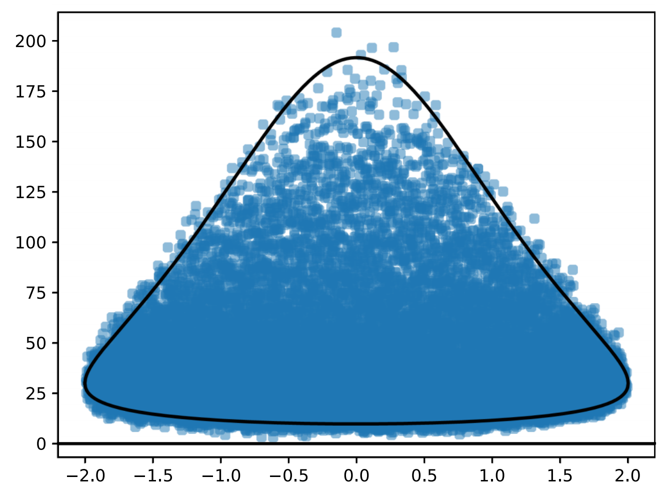

(b) $M = L = 100$, $g = 1.25$ and $g_0 = 5.05$

FIG. 1. Eigenvalues of five 4000×4000 matrices, with the solid line indicating Eqs. (15) (a) and (17) (b).

We also record for completeness the general expression for the density of zeros, valid for any M, L:

$$\widetilde{\rho}(x, y) = \frac{1}{(g+g_0)^{M+L-1}} \int_{-1}^{1} du\, e^{-2uy}(g+u)^M (g_0 - u)^L \times \left\{ \theta(-y) e^{2g_0 y} \sum_{n=1}^{L} a_n(L, M) \frac{[-2(g+g_0)y]^{n-1}}{\Gamma(n)} + \theta(y) e^{-2gy} \sum_{n=1}^{M} a_n(M, L) \frac{[2(g+g_0)y]^{n-1}}{\Gamma(n)} \right\}, \tag{19}$$

where

$$a_n(M, L) = \frac{\Gamma(M+L-n)}{\Gamma(M-n+1)\Gamma(L)}. \tag{20}$$

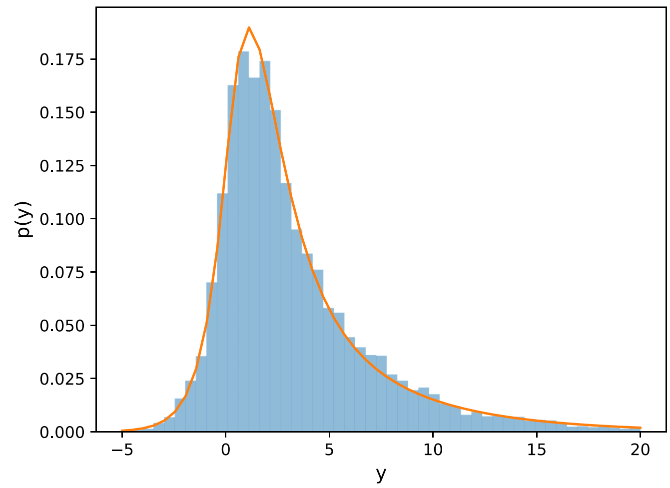

(a) $N = 100$, $M = 4$, $L = 2$

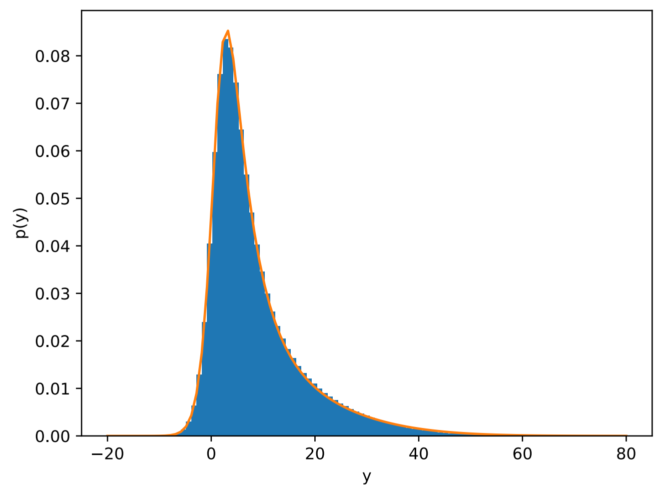

(b) $N = 500$, $M = 10$, $L = 5$

FIG. 2. Density of the imaginary parts $\mathrm{Im} z_n$ for $\mathrm{Re} z_n = 0$ compared against (19) (solid line).

The above mean density in y for $x = 0$ is compared with RMT simulations in Figs. 2(a) and 2(b).

III. STATISTICS OF REFLECTION TIME DIFFERENCE FOR SYSTEMS WITH BROKEN TIME-REVERSAL INVARIANCE

In this section, we convert the information about S-matrix zeros into information about the two-point connected correlation function of the reflection time difference $\delta\mathcal{T}$ defined via (10). In doing this, we largely follow the method proposed in [74] for the Wigner time delays. We start by recalling that the main microscopic energy scale characterizing (real) eigenvalues of the Hermitian RMT cavity Hamiltonian H_0 is the associated mean level spacing $\Delta = [N\nu(E)]^{-1}$, and we introduce the appropriately rescaled RTD via $\widetilde{\delta\mathcal{T}} = \frac{\Delta}{2\pi}\delta\mathcal{T}$. From a technical point of view it is more natural to consider the associated Fourier transform of the two-point correlation function in question defined as

$$C_{M,L}(t) := \frac{1}{2\pi}\int d\omega\, e^{i\omega t}\left\langle \widetilde{\delta\mathcal{T}}\left(E+\frac{\Delta}{2\pi}\omega\right)\widetilde{\delta\mathcal{T}}\left(E-\frac{\Delta}{2\pi}\omega\right)\right\rangle_c. \tag{21}$$

Defining the so-called empirical density of S-matrix zeros z_n in the complex plane $z = \mathrm{Im}z + i\,\mathrm{Re}z$ as

$$\rho(z) = \frac{1}{N}\sum_{n=1}^{N}\delta^{(2)}(z-z_n), \tag{22}$$

where $\delta^{(2)}(z-z_n) := \delta(\mathrm{Re}z-\mathrm{Re}z_n)\delta(\mathrm{Im}z-\mathrm{Im}z_n)$, with $\delta(x)$ being the standard Dirac delta function, we first rewrite (10) as

$$\widetilde{\delta\mathcal{T}}(E) = \frac{\Delta N}{2\pi}\int \frac{2\,\mathrm{Im}z}{(E-\mathrm{Re}z)^2+(\mathrm{Im}z)^2}\,\rho(z)\; d\,\mathrm{Re}z\, d\,\mathrm{Im}z, \tag{23}$$

and then we substitute this in (21) and perform the ensemble-averaging. In doing this, we exploit the relation between covariance functions of empirical densities and the two-point function featured in (11) for $n=2$, hence the associated kernel (12):

$$\langle\rho(z_1)\rho(z_2)\rangle_c = \langle\rho(z_1)\rangle\delta(z_1-z_2) - \mathcal{Y}_2(z_1,z_2), \tag{24}$$

where $\mathcal{Y}_2(z_1,z_2) = |K(z_1,z_2^*)|^2$ is the associated two-point "cluster" function. After rescaling and straightforward manipulations, this brings (21) to the form

$$C_{M,L}(t>0) = A(t)-B(t), \quad A(t) = \frac{1}{2}\int dy\, e^{-2|y|t}\tilde{\rho}(E,y) \tag{25}$$

and

$$B(t) = \frac{1}{2\pi}\int d\omega dy_1 dy_2\, e^{-it\omega-(|y_1|+|y_2|)t} \tag{26}$$

$$\times\mathcal{Y}_2(E,\omega,y_1,y_2)\,\mathrm{sgn}(y_1y_2).$$

Finally, using the expression (12) for the kernel, we arrive at the following formulas:

$$A(t) = \frac{1}{4}\int_{-1}^{1} du\frac{(g+u)^M(g_0-u)^L}{(g+g_0)^{M+L}} \times\left[\sum_{n=1}^{M}a_n(M,L)\left(\frac{g+g_0}{g+t+u}\right)^n + \sum_{n=1}^{L}a_n(L,M)\left(\frac{g+g_0}{g_0+t-u}\right)^n\right], \tag{27}$$

$$B(t) = \frac{\theta(2-t)}{4}\int_{-1}^{1-t} du\frac{(g+u)^M(g_0-u)^L}{(g+g_0)^{2(M+L)}}(g+t+u)^M \times(g_0-t-u)^L\left[\sum_{n=1}^{M}a_n(M,L)\left(\frac{g+g_0}{g+t+u}\right)^n - \sum_{n=1}^{L}a_n(L,M)\left(\frac{g+g_0}{g_0-u}\right)^n\right]^2, \tag{28}$$

where $a_n(L,M)$ has been defined in (20).

A few remarks are in order. First, the limit of no absorption is equivalent to sending $g_0\to\infty$. The dominant contribution then obviously comes from the $n=M$ term in the first sum, in both $A(t)$ and $B(t)$. The resulting expression reproduces the well-known correlation function of the Wigner time delay for systems with broken time-reversal invariance [33,59]:

$$C_{M,0}(t) = \frac{1}{4}\int_{\max(1-t,-1)}^{1}\left(\frac{g+u}{g+t+u}\right)^M du. \tag{29}$$

Note that the above correlation function of Wigner time delays decays as t^{-M} for $t\to\infty$, whereas the corresponding correlation of RTD for any finite absorption $g_0<\infty$ decays in the same limit as t^{-1} for any fixed value $M>0, L>0$. This implies that the variance of the RTD, which in view of (21) can be found as

$$\langle[\widetilde{\delta\mathcal{T}}(E)]^2\rangle_c \propto \int_0^\infty C_{M,L}(t)dt,$$

logarithmically diverges for any finite number of absorbing channels. This feature is strikingly different from the Wigner time delay, whose variance is infinite only for a single-channel scattering, being finite for any $M>1$. The logarithmic divergence of the variance suggests that the distribution of RTD must have the large-tail behavior $P(\widetilde{\delta\mathcal{T}})\sim\widetilde{\delta\mathcal{T}}^{-3}$. Although we cannot prove this conjecture rigorously in general, it can be strongly supported by a perturbative argument (sketched in the Appendix) valid in the regime of small absorption in a weakly open system with equivalent channels, $\gamma_a=\gamma\ll 1$, $\rho_a=\rho\ll 1$, when imaginary parts of the S-matrix zeros are much smaller than their separation: $\langle|\mathrm{Im}z_n|\rangle\ll\Delta$. Adapting the argument along the lines used in [33] for Wigner time delays, and further assuming $\rho\gtrsim\gamma$, the probability density for RTD can be shown to have an algebraic decay with universal exponents,

$$P_\beta(\widetilde{\delta\mathcal{T}})\sim\begin{cases}|\widetilde{\delta\mathcal{T}}|^{-3/2}, & 1\ll|\widetilde{\delta\mathcal{T}}|\ll\gamma^{-1},\\ |\widetilde{\delta\mathcal{T}}|^{-3}, & |\widetilde{\delta\mathcal{T}}|\gg\gamma^{-1},\end{cases} \tag{30}$$

and similarly for negative $\widetilde{\delta\mathcal{T}}$ with γ and ρ exchanging their roles. This result is "superuniversal," that is, it holds not only for systems with broken symmetry but for all standard symmetry classes of H_0 described by values of the Dyson index $\beta=1,2,4$ and for all $M>0, L>0$. We indeed see that the infinite variance is due to the cubic asymptotic decay in the probability density. Note that in the case of Wigner time delay τ the asymptotic tail of the probability density is rather $\tau^{-\beta M/2-2}$ making the variance finite for $M>2/\beta$. Anticipating that for $\rho=0$ RTD should be indistinguishable from the Wigner time delay, one may consider the parameter range $\rho\ll\gamma$ and find that in that case the decay $\widetilde{\delta\mathcal{T}}^{-\beta M/2-2}$ also happens for RTD in the intermediate asymptotic range $1/\gamma\ll\widetilde{\delta\mathcal{T}}\ll 1/\rho$, whereas the cubic tail takes over only as $\widetilde{\delta\mathcal{T}}\gg 1/\rho$, reconciling the two types of behavior.

One can also be interested in the short-time behavior of the RTD correlation function. Considering for simplicity the simplest case $M = L = 1$, we obtain in this limit

$$C_{1,1}(t \ll 1) = \frac{1}{2}\left[1 - \frac{4+3(g-g_0)^2}{3(g+g_0)^2}\right] + \frac{(g-g_0)^2 - 4(g+g_0-1)}{4(g+g_0)^2}t + O(t^2). \quad (31)$$

The first-order term vanishes when $g_0^{\pm} = g + 2 \pm 2\sqrt{2g}$ and vice versa. For $1 < g < 3 + 2\sqrt{2}$, the second solution $g_0^- = g + 2 - 2\sqrt{2g} < 1$ is not valid since $g, g_0 > 1$ by definition. Thus, the correlator switches from an increasing to a decreasing function of time as g_0 passes through g_0^+. Reverting to the frequency domain, we find that in this case the correlator decays as ω^{-4}, whereas the correlator of the Wigner time delay always decays as ω^{-2} since $\dot{C}_{M,0}(0) = 1/4$.

Another curious observation is that due to the appearance of the factor $\text{sgn}(y_1 y_2)$ in the integrand of (32), the term $B(t)$ identically vanishes when $\mathcal{Y}_2$ is even in y_1 and y_2 separately, in which case $C(t)$ only depends on the mean global density of complex eigenvalues rather than on the two-point correlation function. For equivalent channels, a necessary condition for this to happen is $M = L$ and $g = g_0$.

To compare with numerical simulations, we find that instead of directly computing (21), it is more practical to consider instead the Fourier transform of the RTD weighted by a Gaussian:

$$F(t, W) := \int \frac{dE}{\sqrt{2\pi W}} \delta\widetilde{\mathcal{T}}(E) e^{iEt - \frac{E^2}{2W}} \quad (32)$$

$$= \sqrt{\frac{\pi}{2W}} e^{-\frac{Wt^2}{2}} \sum_{n=1}^{N} \text{sgn}(\text{Im} z_n) \times \left[\text{erfcx}\left(\frac{|\text{Im} z_n| + Wt + i\,\text{Re} z_n}{\sqrt{2W}}\right) + \text{erfcx}\left(\frac{|\text{Im} z_n| - Wt - i\,\text{Re} z_n}{\sqrt{2W}}\right)\right], \quad (33)$$

where $\text{erfcx}(z) = e^{z^2}\text{erfc}(z)$, and $\text{erfc}(z) = \frac{2}{\sqrt{\pi}} \int_z^\infty e^{-x^2} dx$ is the complementary error function. If we take $\frac{1}{N} \ll \sqrt{W} \ll 1$, then we find the approximate relation

$$\frac{\Delta}{4\pi}\sqrt{\frac{W}{\pi}} \langle |F\left(\frac{\pi t}{\Delta}; W\right)|^2 \rangle_c \approx C_{M,L}(t). \quad (34)$$

The advantage of this approach is that the ensemble average of $F(t; W)$ converges faster than that of the RTD. Figures 3(a) and 3(b) compare the correlator obtained in this way from RMT simulations ($N = 300$) with the prediction for $M = 1$ and $L = 0, 1$.

IV. ON EXTRACTING S-MATRIX ZEROS FROM SCATTERING DATA

Let us now discuss a possibility of determining the positions of the zeros of a subunitary scattering matrix from an experiment, real or numerical. One may imagine two possibilities: either one has access to the total unitary S matrix, or only to its subunitary observable/scattering block $S(E)$. Indeed, one may consider constructing a CPA in the form of a three-port microwave network, where one port plays the role of the attenuator providing absorption. In such a setup, if one disregards imperfections in the setup, the output in all three ports is directly accessible, hence the total S matrix.

In the usual case of S-matrix poles, one of the most well-established methods for determining their positions in the lower half-plane is "harmonic inversion" [44], which estimates the poles by solving a set of nonlinear equations. Basically, one estimates a signal represented in the time domain as a sum of decaying exponentials evaluated at times $t = n\tau$, where τ is the sample rate, by relying on the Padé

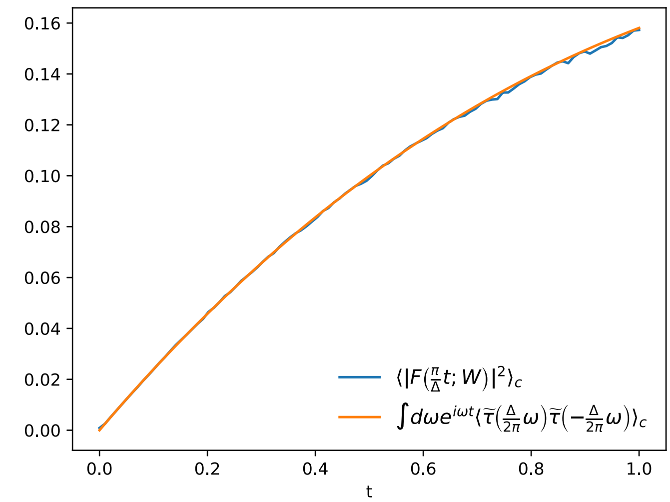

(a) $M = 1, L = 0, g = 1.25$

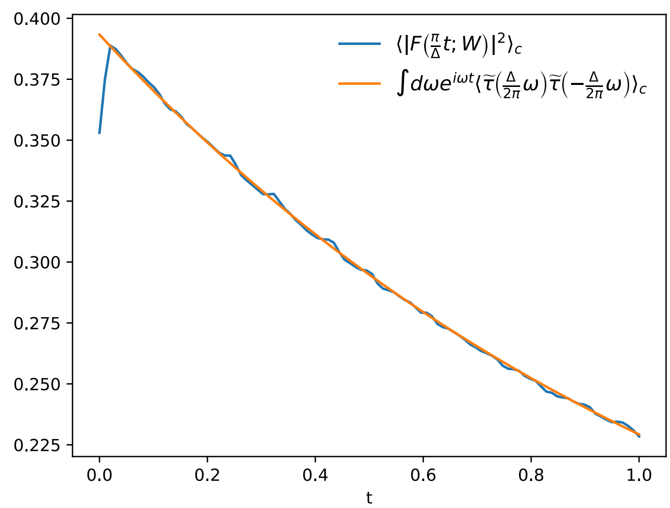

(b) $M = 1, L = 1, g = g_0 = 1.25$

FIG. 3. $C_{M,L}(t)$ of (21) compared with simulations of 300×300 random matrices, using (34) as an estimator. The small time discrepancy in the second figure appears to be a finite-size effect that occurs over a smaller window in time as the dimension of the matrices increases.

approximation:

$$c_n := \sum_{k=1}^{N} d_k e^{-iz_k n\tau}, \tag{35}$$

$$f(z) := \sum_{n=0}^{\infty} c_n z^{-n} = \sum_{k=1}^{N} \frac{d_k z_k}{z - z_k} \tag{36}$$

$$= \frac{P_K(z)}{Q_K(z)}, \tag{37}$$

where P_K/Q_K is the order (K, K) Padé approximant to $f(z)$. The zeros z_k are the poles of $Q(z)$, and the amplitudes d_k are the ratio of the residues and the poles. The integer K is chosen as an upper bound to the number of true zeros N, leading to $N - K$ spurious zeros that must be discarded. In general, it is common to introduce a cutoff and discard zeros for which the magnitude of the residue falls below the cutoff. The procedure for S-matrix poles outlined in [43] used a cutoff and discarded those poles whose imaginary parts were smaller than the energy spacing (distance between energy samples), as well as with real parts near the boundary of the sampling window.

Harmonic inversion can be performed directly on the S-matrix elements or, alternatively, on the Wigner time delay. When estimating zeros, the signal to be considered is given by the inverse of the determinant:

$$\frac{1}{\det S(E)} = \prod_{n=1}^{N} \frac{E - E_n + i\Gamma_n/2}{E - \mathrm{Re} z_n - i\,\mathrm{Im} z_n}. \tag{38}$$

Alternatively, when the whole unitary $\mathcal{S}$ can be measured, one can use the expression (10) for the RTD. Assuming additionally a weak uniform absorption $\epsilon \ll 1$ inside the scattering domain, the RTD can be alternatively computed from the unitary deficit of the determinant ratio (see [56] for a discussion):

$$\delta\mathcal{T}(E) = -\frac{1}{\epsilon}\mathrm{Re}\ln\frac{\det S(E + i\epsilon)}{\det S'(E + i\epsilon)} + O(\epsilon^2). \tag{39}$$

The advantage of using the RTD for extracting positions of complex zeros is that the Lorentzians in the sum are all normalized to unity, providing us with a way to distinguish true and spurious zeros by looking at the corresponding residues. The residues in (38) involve instead a product over the remaining zeros and poles which can take arbitrary values. It is not *a priori* clear how to choose an appropriate cutoff, particularly when the zeros/poles appear as Lorentzians with varying amplitudes. We compare the performance of both methods for extracting the zeros by simulating H_0 from the GUE; parameters affecting the accuracy of the estimates are the number of samples nE of $S(E)$ and the strength of the uniform absorption ϵ. Since the first step of the harmonic inversion procedure is to take the Fourier transform, when using (38) we perform a second transform on the complex conjugate so that the zeros in both half-planes are accounted for. The detection of spurious zeros differs between the two methods. In the first method, we follow [43] in using a cutoff and removing zeros near the boundaries. The cutoff has been chosen as 1, the value accounting well for most of the spurious zeros. In the second method, the zeros occur in complex conjugate pairs whose residues (after normalizing by the energy spacing) should add up to 1. We therefore grouped the zeros into conjugate pairs and removed those whose residues were significantly different from 1. This allowed us to bypass the need for the removal of zeros near the boundaries. Figure 4 shows the true zeros plotted against those estimated from (38) and (39), for various parameter configurations. In Figs. 4(a) and 4(c), there are what appear to be spurious zeros (isolated green crosses) among those estimated by the second method. These arise because of the appearance of two complex conjugate pairs for the same zero; in general, we observe that as the strength of the uniform absorption ϵ increases, an increasing number of zeros are associated with two or more complex conjugate pairs. This is why these do not appear in Figs. 4(b) and 4(d), where $\epsilon = 10^{-6}$. One could attempt to group all pairs in order to bring the sum of residues closer to 1, or simply discard all but one pair. Note also that in all four figures there are zeros near the boundaries that are discarded in the first method but included in the second.

V. DISCUSSION AND OPEN PROBLEMS

In conclusion, we have studied the statistics of the zeros of the subunitary S matrix for a RMT-based model of scattering in chaotic cavities with localized absorption and broken time-reversal symmetry. The n-point correlation functions of the zeros in the complex plane for a system with a finite number of scattering and absorbing channels (M and L, respectively) can be calculated by extending the method used in [34] for characterizing the S-matrix poles (formally equivalent to the $L = 0$ case). The resulting kernel, in the limit of strong non-Hermiticity with at least one of the parameters M and/or L going to infinity, takes the form of a generalized Ginibre kernel, expected to be universal in this regime [39]. For finite $M < \infty$ and $L < \infty$, the kernel was used to obtain the Fourier transform of the correlation function $C_{M,L}(t)$ of the RTD, which has been shown to decay as $C_{M,L}(t) \sim t^{-1}$ at large times for any $L > 0$. This is in sharp contrast with the case $L = 0$ (formally equivalent to replacing RTD with the Wigner time delay), where a similar tail is known to be M-dependent: $\sim t^{-M}$. In particular, this implies that the variance of the RTD is infinite regardless of the value of M or L. We interpret this divergence as evidence for the existence of a far tail $P(\widetilde{\delta\mathcal{T}}) \sim \delta\mathcal{T}(E)^{-3}$ in the RTD probability density, and we verify this in the regime of a weakly open and weakly absorbing system. We expect such a tail to be a superuniversal feature of the RTD distribution valid for all symmetry classes.

The short-time behavior of the RTD correlation function is again markedly different for $L = 0$ and $L > 0$: $C_{M,0}(t) \sim \frac{1}{4}t$ in the former case and $C_{M,L}(t) \sim C_{M,L}(0) + \dot{C}_{M,L}(0)t$ in the latter, with $C_{M,L}(0) \neq 0$ and the coefficient $\dot{C}_{M,L}(0)$ depending on g and g_0 in such a way that it changes from a positive value through zero to negative values as g_0 is reduced from infinity toward unity. This implies that there must exist a particular value of absorption parameter g_0 (depending on g) such that the large frequency asymptotic of the Fourier-transformed correlation function decays as ω^{-4} instead of the typical decay ω^{-2}.

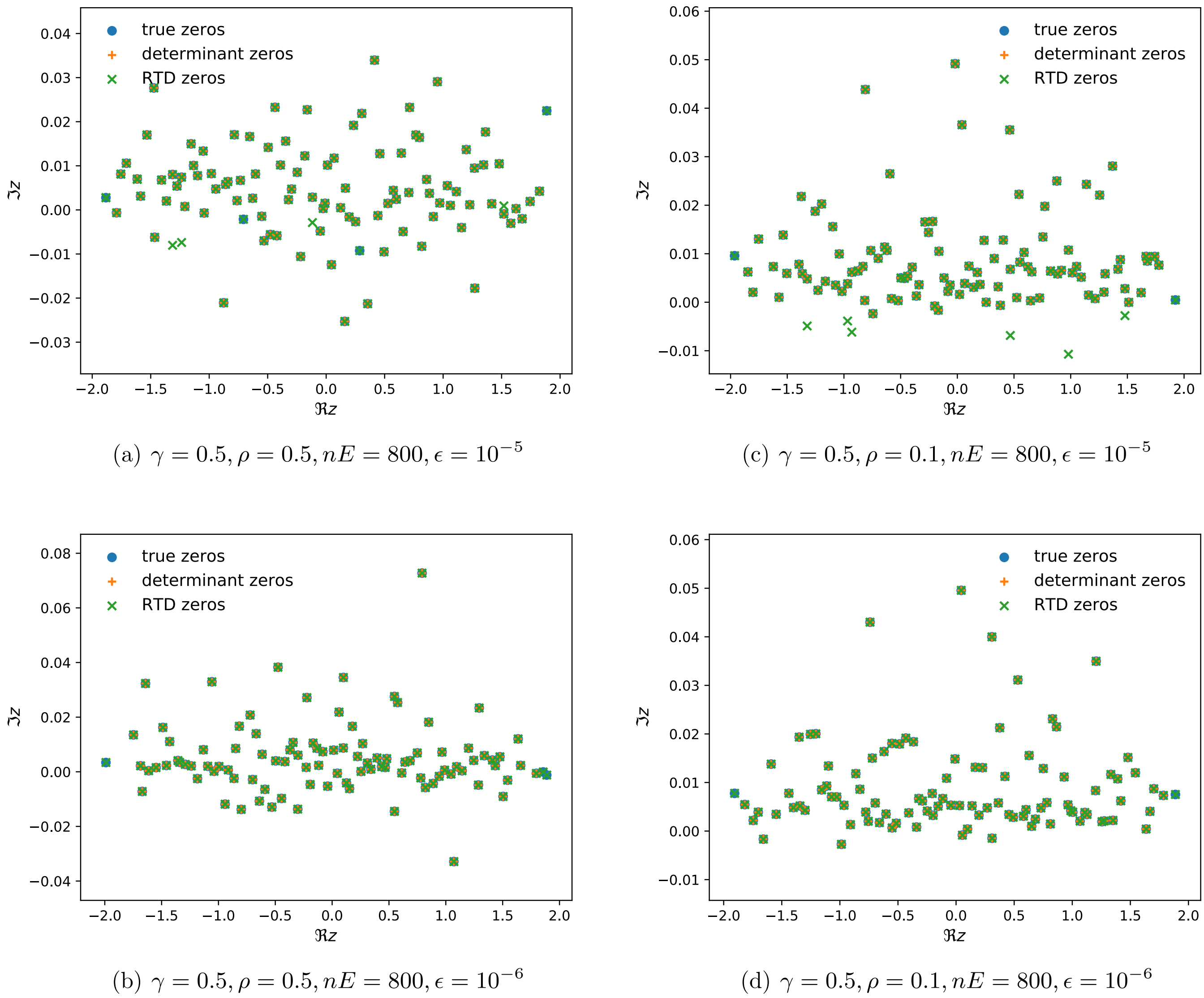

(a) $\gamma = 0.5, \rho = 0.5, nE = 800, \epsilon = 10^{-5}$

(c) $\gamma = 0.5, \rho = 0.1, nE = 800, \epsilon = 10^{-5}$

(b) $\gamma = 0.5, \rho = 0.5, nE = 800, \epsilon = 10^{-6}$

(d) $\gamma = 0.5, \rho = 0.1, nE = 800, \epsilon = 10^{-6}$

FIG. 4. Estimated zeros using (38) (orange plus signs) and (39) (green crosses) compared to true zeros (blue circles). In all cases, $N = 100, M = 2, L = 1$.

We have also examined two methods for extracting the positions of S-matrix zeros from experimental scattering data by harmonic inversion of either the inverse determinant of S or from the RTD. The first method is applicable when only the scattering part of S is available, while for the second method the total S-matrix must be accessible. The advantage of the second method is that we know in advance the residue of each zero, which allows us to distinguish more easily between true and spurious zeros. In the recent papers demonstrating the construction of a disordered CPA [26,27], the S-matrix was measured at regular intervals in an energy window, but rather than determine the zeros, each S-matrix was diagonalized and the eigenvalue closest to zero selected as a candidate for the CPA state. Using harmonic inversion, one can instead directly estimate the zeros themselves.

Finally, let us mention that all nonperturbative treatment in our paper has been restricted to systems with broken time-reversal invariance. Actually, the mean density of complex eigenvalues z_n for chaotic systems with preserved time-reversal invariance, with H_0 being taken from the Gaussian orthogonal ensemble, can be deduced for $L > 0$ from known $L = 0$ results by an ad hoc analytic continuation; see [29]. However, its systematic controllable derivation, not speaking about deducing the form of the two-point (and higher) correlation functions, remains an outstanding and challenging problem. This currently prevents us from any nonperturbative insights into the statistics of the reflection time difference (apart from its expected superuniversal cubic tail in the probability density) for this important case.

ACKNOWLEDGMENTS

We thank Mikhail Poplavskyi for sharing his notes about the derivation of (A6), and Steven Anlage for his interest in the project and valuable discussions of this and related topics. M.O. acknowledges funding from the EPSRC Centre for Doctoral Training in Cross-Disciplinary Approaches to Non-Equilibrium Systems (CANES) under Grant No. EP/L015854/1.

APPENDIX

Derivation of the correlation function of S-matrix zeros

We give a brief sketch of the derivation of the expression (12) for the n-point correlation function. Since the derivation follows mainly the steps of [34] (explained in more detail in [39]), we omit the detail and point out only the necessary modification. The object of study is the spectrum of the perturbed GUE matrix $J = H + i\Gamma$, where $\Gamma = \mathrm{diag}(\gamma_1, \dots, \gamma_{M+L}, 0, \dots, 0)$ is a rank $M + L$ matrix where $\gamma_1 \geqslant \cdots \geqslant \gamma_M > 0 > \gamma_{M+1} \geqslant \cdots \gamma_{M+L}$. It is the fact that the matrix Γ has eigenvalues of both signs that makes a difference from [34] and should be properly accounted for. The joint probability density for the matrix J induced by H is

$$P(J)dJ \propto e^{-\frac{N}{2}\mathrm{tr}(\frac{J+J^\dagger}{2})^2}\delta\left(\frac{J-J^\dagger}{2i} - \Gamma\right), \tag{A1}$$

where $\delta(A) = \prod_{i,j}\delta(A_{ij})$. Making use of the Schur decomposition $J = U(Z + R)U^\dagger$, the integral over the upper triangular matrix R can be performed with the δ function in the off-diagonal elements. The remaining δ functions in the diagonal elements are represented by a Fourier integral over a diagonal matrix K, leaving a Harish-Chandra–Itzykson–Zuber (HCIZ) integral with K and Γ. Since Γ is not of full rank, the limit of $N - M - L$ eigenvalues going to zero is calculated by repeated application of l'Hôpital's rule to the original HCIZ formula. The result is the following expression for the density of eigenvalues Z:

$$P(Z) \propto \frac{|\Delta(Z)|^2}{\det^{N-M-L}(\gamma)\Delta(\gamma)}e^{-\frac{N}{2}\mathrm{Re}\mathrm{tr}Z^2 - \frac{N}{2}\mathrm{tr}\gamma^2} \times \int \frac{dK}{(2\pi)^N}\frac{e^{i\mathrm{tr}K\,\mathrm{Im}Z}}{\Delta(K)}\mathcal{D}(K), \tag{A2}$$

where we denoted $\gamma = \mathrm{diag}(\gamma_1, \dots, \gamma_{M+L})$ and introduced

$$\mathcal{D}(K) := \det\begin{vmatrix} e^{-ik_1\gamma_1} & \cdots & e^{-ik_1\gamma_{M+L}} & (-ik_1)^{N-M-L-1} & \cdots & 1 \\ \vdots & \ddots & \vdots & \vdots & \ddots & \vdots \\ e^{-ik_N\gamma_1} & \cdots & e^{-ik_N\gamma_{M+L}} & (-ik_N)^{N-M-L-1} & \cdots & 1 \end{vmatrix}. \tag{A3}$$

The difference now from the original derivation is that the terms $e^{-ik_j\gamma_c}$ are represented by the integral

$$e^{-ik_j\gamma_c} = \frac{1}{2\pi i}\int_{\mathcal{L}_c}\frac{e^{-ik_j\lambda_c}}{\lambda_c - k_j}d\lambda_c, \tag{A4}$$

where $\mathcal{L}_c = \mathrm{sgn}(\gamma_c)(-\mathbb{R} + i0)$. After taking the λ integrals outside the determinant and using the following identity:

$$\det\begin{vmatrix} \frac{1}{\lambda_1-k_1} & \cdots & \frac{1}{\lambda_{\mathcal{M}}-k_1} & (-ik_1)^{N-\mathcal{M}-1} & \cdots & 1 \\ \vdots & \ddots & \vdots & & \ddots & \vdots \\ \frac{1}{\lambda_1-k_N} & \cdots & \frac{1}{\lambda_{\mathcal{M}}-k_N} & (-ik_N)^{N-\mathcal{M}-1} & \cdots & 1 \end{vmatrix} \propto \frac{\Delta(\Lambda)\Delta(K)}{\prod_{j=1}^{\mathcal{M}}\prod_{i=1}^{N}(\lambda_j - k_i)}, \tag{A5}$$

which follows by elementary row and column operations, the final expression for the density $P(Z)$ is

$$P(Z) \propto \frac{1}{\det^{N-\mathcal{M}}(\gamma)\Delta(\gamma)}|\Delta(Z)|^2 e^{-\frac{N}{2}\mathrm{Re}\mathrm{tr}Z^2 - \frac{N}{2}\mathrm{tr}\gamma^2} \times \int_{\mathcal{L}_1}\cdots\int_{\mathcal{L}_{\mathcal{M}}} d\Lambda\,\Delta(\Lambda)e^{-i\sum_{j=1}^{\mathcal{M}}\gamma_j\lambda_j} \times \prod_{i=1}^{N}\sum_{j=1}^{\mathcal{M}}\frac{e^{i\lambda_j\mathrm{Im}z_i}}{\prod_{l\neq j}(\lambda_l - \lambda_j)}\theta(\mathrm{Im}\lambda_j\mathrm{Im}z_i), \tag{A6}$$

where $\mathcal{M} = M + L$. The above expression is exact for any N, M, L with $M + L < N$, but in order to make further progress in deriving the n-point correlation function, we consider the limit of weak non-Hermiticity when $N \to \infty$ with M, L, n finite, for which the results are expected to be broadly independent of the model details [39,81]. From this point onward, the derivation follows exactly along the lines of [39], where in the Appendix of that paper the n-point correlation function is related to the average of a product of characteristic polynomials that is subsequently evaluated by integrating over anticommuting variables.

Distribution of RTD in the regime of weak coupling and absorption

In this regime, the imaginary part of the zeros is much smaller than the typical separation between the real parts, and, moreover, the imaginary parts of neighboring zeros are independent to leading order. Then the dominant contribution to RTD at a given real energy E can be estimated by a heuristic argument [33] that takes into account only the zero whose real part is the closest to the energy value E in the sum of Lorentzians (10). Attributing the index n to this particular zero and defining $u_n = \frac{\beta\pi}{\Delta}(E - \mathrm{Re}z_n)$ and $y_n = \frac{\beta\pi}{\Delta}\mathrm{Im}z_n$, we have

$$\widetilde{\delta\mathcal{T}}(E) \simeq \frac{2y_n}{u_n^2 + y_n^2}. \tag{A7}$$

The real and imaginary parts of z_n are independent in the weak-coupling regime, with the latter having the density

$$P_Y^\beta(y) = \int\frac{dk}{2\pi}\frac{e^{iky}}{\prod_{a=1}^{M}(1 + 2ik\gamma_a)^{\beta/2}\prod_{b=1}^{L}(1 - 2ik\rho_b)^{\beta/2}}. \tag{A8}$$

We also assume that u_n is uniformly distributed in $[-\beta\pi, \beta\pi]$. The result of these approximations is the following estimate for the density of $\widetilde{\delta\mathcal{T}} \equiv \tau$:

$$P^{\beta}_{\widetilde{\delta\mathcal{T}}}(\tau) = \int dy\, P_\beta(y) \int_{-\beta\pi}^{\beta\pi} du\, \delta\left(\tau - \frac{2y}{u^2+y^2}\right) \tag{A9}$$

$$\simeq \frac{2}{\tau^3}\int_0^{\min(1,\frac{\beta^2\pi^2\tau^2}{4})} \sqrt{\frac{y}{1-y}}\left[\theta(\tau)P_Y^\beta\left(\frac{2y}{\tau}\right) + \theta(-\tau)P_Y^\beta\left(-\frac{2y}{\tau}\right)\right]dy. \tag{A10}$$

Focusing on positive $\widetilde{\delta\mathcal{T}}$ and equivalent channels $\gamma_a = \gamma \ll 1$, $\rho_b = \rho \ll 1$, let us first assume that $\rho \gtrsim \gamma$. Then we can identify two regimes for $\tau > 2/(\beta\pi)$: (i) $\tau\gamma \ll 1$ and (ii) $\tau\gamma \gg 1$. In the first regime, the dominant term in $P_Y^\beta[2y/(M\tau)]$ is $y^{\beta M/2-1}e^{-\frac{y}{\tau\gamma}}$:

$$P^{\beta}_{\widetilde{\delta\mathcal{T}}}(\tau) \simeq \frac{\gamma^{\beta L/2-1}}{\tau^3\Gamma(\beta M/2)(\gamma+\rho)^{\beta L/2}} \times \int_0^\infty \sqrt{y}\left(\frac{y}{\tau\gamma}\right)^{\beta M/2-1} e^{-\frac{y}{\tau\gamma}}dy \tag{A11}$$

$$= \frac{\gamma^{\beta(L+1)/2}}{(\gamma+\rho)^{\beta L/2}}\tau^{-3/2}, \tag{A12}$$

where we have set the upper limit of integration to infinity and taken $1-y \simeq 1$, both justified by the exponential damping. In the second regime, the dominant term is now just $e^{-\frac{y}{\tau\gamma}}$, which is approximately unity,

$$P^{\beta}_{\widetilde{\delta\mathcal{T}}}(\tau) \simeq \frac{\Gamma(\beta(M+L)/2-1)}{\Gamma(\beta M/2)\Gamma(\beta L/2)}\frac{1}{\tau^3\gamma^{\beta M/2}\rho^{\beta L/2}} \times \left(\frac{\gamma\rho}{\gamma+\rho}\right)^{\beta(M+L)/2-1}\int_0^1\sqrt{\frac{y}{1-y}} \tag{A13}$$

$$= \frac{\pi\Gamma(\beta(M+L)/2-1)}{2\Gamma(\beta M/2)\Gamma(\beta L/2)} \times \frac{1}{\gamma^{\beta M/2}\rho^{\beta L/2}}\left(\frac{\gamma\rho}{\gamma+\rho}\right)^{\beta(M+L)/2-1}\tau^{-3}. \tag{A14}$$

Thus we see that $P^{\beta}_{\widetilde{\delta\mathcal{T}}}(\tau)$ behaves as a power law with universal exponents, summarized in (30).

If, however, one assumes $\rho \ll \gamma$ and repeats the analysis above, one finds that the regime $\tau \gg 1/\gamma$ should be further subdivided into two new regimes: $1/\gamma\tau \ll 1/\rho$ and $\tau \gg 1/\rho$. Only in the latter case does one reproduce the superuniversal asymptotics $P^{\beta}_{\widetilde{\delta\mathcal{T}}}(\tau) \simeq \tau^{-3}$, whereas in the former the asymptotic is changed to $P^{\beta}_{\widetilde{\delta\mathcal{T}}}(\tau) \simeq \tau^{-(2+\beta M/2)}$. This type of tail behavior is precisely one that is typical for the Wigner time delays, to which the RTD formally reduces as $\rho \to 0$. The same arguments can be made for negative $\widetilde{\delta\mathcal{T}}$ by exchanging the role of γ with that of ρ.

[1] U. Kuhl, O. Legrand, and F. Mortessagne, Microwave experiments using open chaotic cavities in the realm of the effective Hamiltonian formalism, Fortschr. Phys. **61**, 404 (2013).

[2] G. Gradoni, J.-H. Yeh, B. Xiao, T.-M. Antonsen, S.-M. Anlage, and E. Ott, Predicting the statistics of wave transport through chaotic cavities by the Random Coupling Model: A review and recent progress, Wave Motion **51**, 606 (2014).

[3] B. Dietz and A. Richter, Quantum and wave dynamical chaos in superconducting microwave billiards, Chaos **25**, 097601 (2015).

[4] H. Cao and J. Wiersig, Dielectric microcavities: Model systems for wave chaos and non-Hermitian physics, Rev. Mod. Phys. **87**, 61 (2015).

[5] G. E. Mitchell, A. Richter, and H. A. Weidenmueller, Random matrices and chaos in nuclear physics: Nuclear reactions, Rev. Mod. Phys. **82**, 2845 (2010).

[6] Y. V. Fyodorov and D. V. Savin, Resonance scattering of waves in chaotic systems, in *The Oxford Handbook of Random Matrix Theory*, edited by G. Akemann, J. Baik, and P. Di Francesco (Oxford University Press, Oxford, 2011).

[7] H. Schomerus, Random matrix approaches to open quantum systems, in *Les Houches Summer School on "Stochastic Processes and Random Matrices," 2015*, edited by G. Schehr (Oxford University Press, Oxford, 2017).

[8] R. Schaefer, T. Gorin, T. H. Seligman, and H.-J. Stoeckmann, Correlation functions of scattering matrix elements in microwave cavities with strong absorption, J. Phys. A **36**, 3289 (2003).

[9] R. A. Mendez-Sanchez, U. Kuhl, M. Barth, C. V. Lewenkopf, and H.-J. Stöckmann, Distribution of Reflection Coefficients in Absorbing Chaotic Microwave Cavities, Phys. Rev. Lett. **91**, 174102 (2003).

[10] S. Hemmady, X. Zheng, E. Ott, T. M. Antonsen, and S. M. Anlage, Universal Impedance Fluctuations in Wave Chaotic Systems, Phys. Rev. Lett. **94**, 014102 (2005).

[11] S. Hemmady, X. Zheng, J. Hart, T. M. Antonsen, E. Ott, and S. M. Anlage, Universal properties of two-port scattering, impedance, and admittance matrices of wave-chaotic systems, Phys. Rev. E **74**, 036213 (2006).

[12] X. Zheng, S. Hemmady, T. M. Antonsen, Jr., S. M. Anlage, and E. Ott, Characterization of fluctuations of impedance and scattering matrices in wave chaotic scattering, Phys. Rev. E **73**, 046208 (2006).

[13] O. Hul, O. Tymoshchuk, S. Bauch, P. M. Koch, and L. Sirko, Experimental investigation of Wigner's reaction matrix for irregular graphs with absorption, J. Phys. A **38**, 10489 (2005).

[14] M. Lawniczak, O. Hul, S. Bauch, P. Seba, and L. Sirko, Experimental and numerical investigation of the reflection coefficient and the distributions of Wigner's reaction matrix for irregular graphs with absorption, Phys. Rev. E **77**, 056210 (2008).

[15] M. Lawniczak, S. Bauch, O. Hul, and L. Sirko, Experimental investigation of the enhancement factor for microwave irregular networks with preserved and broken time reversal symmetry in the presence of absorption, Phys. Rev. E **81**, 046204 (2010).

[16] P. W. Brouwer and C. W. J. Beenakker, Voltage-probe and imaginary potential models for dephasing in a chaotic quantum dot, Phys. Rev. B **55**, 4695 (1997).

[17] C. W. J. Beenakker and P. W. Brouwer, Distribution of the reflection eigenvalues of a weakly absorbing chaotic cavity, Physica E **9**, 463 (2001).

[18] Y. V. Fyodorov, Induced vs. spontaneous breakdown of S-matrix unitarity: Probability of no return in quantum chaotic and disordered systems, JETP Lett. **78**, 250 (2003).
[19] Y. V. Fyodorov and D. V. Savin, Statistics of impedance, local density of states, and reflection in quantum chaotic systems with absorption, JETP Lett. **80**, 725 (2004).
[20] D. V. Savin, H. J. Sommers, and Y. V. Fyodorov, Universal statistics of the local Green's function in wave chaotic systems with absorption, JETP Lett. **82**, 544 (2005).
[21] Y. V. Fyodorov, D. V. Savin, and H.-J. Sommers, Scattering, reflection and impedance of waves in chaotic and disordered systems with absorption, J. Phys. A **38**, 10731 (2005).
[22] I. Rozhkov, Y. V. Fyodorov, and R. L. Weaver, Statistics of transmitted power in multichannel dissipative ergodic structures, Phys. Rev. E **68**, 016204 (2003).
[23] I. Rozhkov, Y. V. Fyodorov, and R. L. Weaver, Variance of transmitted power in multichannel dissipative ergodic structure invariant under time reversal, Phys. Rev. E **69**, 036206 (2004).
[24] S. B. Fedeli and Y. V. Fyodorov, Statistics of off-diagonal entries of Wigner K-matrix for chaotic wave systems with absorption, J. Phys. A **53**, 165701 (2020).
[25] Y. D. Chong, L. Ge, H. Cao, and A. D. Stone, Coherent Perfect Absorbers: Time-Reversed Lasers, Phys. Rev. Lett. **105**, 053901 (2010).
[26] K. Pichler, M. Kühmayer, J. Böhm, A. Brandstötter, P. Ambichl, U. Kuhl, and S. Rotter, Random anti-lasing through coherent perfect absorption in a disordered medium, Nature (London) **567**, 351 (2019).
[27] L. Chen, T. Kottos, and S. M. Anlage, Perfect absorption in complex scattering systems with or without hidden symmetries, arXiv:2001.00956.
[28] H. Li, S. Suwunnarat, R. Fleischmann, H. Schanz, and T. Kottos, Random Matrix Theory Approach to Chaotic Coherent Perfect Absorbers, Phys. Rev. Lett. **118**, 044101 (2017).
[29] Y. V. Fyodorov, S. Suwunnarat, and T. Kottos, Distribution of zeros of the S-matrix of chaotic cavities with localized losses and coherent perfect absorption: Non-perturbative results, J. Phys. A **50**, 30LT01 (2017).
[30] V. V. Sokolov and V. G. Zelevinsky, Dynamics and statistics of unstable quantum states, Nucl. Phys. A **504**, 562 (1989).
[31] F. Haake, F. Izrailev, N. Lehmann, D. Saher, and H.-J. Sommers, Statistics of complex levels of random matrices for decaying systems, Z. Phys. B **88**, 359 (1992).
[32] Y. V. Fyodorov and H.-J. Sommers, Statistics of S-matrix poles in few-channel chaotic scattering: Crossover from isolated to overlapping resonances, JETP Lett. **63**, 1026 (1996).
[33] Y. V. Fyodorov and H.-J. Sommers, Statistics of resonance poles, phase shifts and time delays in quantum chaotic scattering: Random matrix approach for systems with broken time-reversal invariance, J. Math. Phys. **38**, 1918 (1997).
[34] Y. V. Fyodorov and B. A. Khoruzhenko, Systematic Analytical Approach to Correlation Functions of Resonances in Quantum Chaotic Scattering, Phys. Rev. Lett. **83**, 65 (1999).
[35] H.-J. Sommers, Y. V. Fyodorov, and M. Titov. S-matrix poles for chaotic quantum systems as eigenvalues of complex symmetric random matrices: From isolated to overlapping resonances, J. Phys. A **32**, L77 (1999).
[36] R. A. Janik, W. Noerenberg, M. A. Nowak, G. Papp, and I. Zahed, Correlations of eigenvectors for non-hermitian random-matrix models, Phys. Rev. E **60**, 2699 (1999).
[37] H. Schomerus, K. M. Frahm, M. Patra, and C. W. J. Beenakker, Quantum limit of the laser line width in chaotic cavities and statistics of residues of scattering matrix poles, Physica A **278**, 469 (2000).
[38] Y. V. Fyodorov and B. Mehlig, Statistics of resonances and nonorthogonal eigenfunctions in a model for single-channel chaotic scattering, Phys. Rev. E **66**, 045202(R) (2002).
[39] Y. V. Fyodorov and H.-J. Sommers, Random matrices close to hermitian or unitary: Overview of methods and results, J. Phys. A **36**, 3303 (2003).
[40] G. L. Celardo, N. Auerbach, F. M. Izrailev, and V. G. Zelevinsky, Distribution of Resonance Widths and Dynamics of Continuum Coupling, Phys. Rev. Lett. **106**, 042501 (2011).
[41] Y. V. Fyodorov and D. V. Savin, Statistics of Resonance Width Shifts as a Signature of Eigenfunction Nonorthogonality, Phys. Rev. Lett. **108**, 184101 (2012).
[42] Y. V. Fyodorov and D. V. Savin, Resonance width distribution in RMT: Weak-coupling regime beyond Porter-Thomas, Europhys. Lett. **110**, 40006 (2015).
[43] U. Kuhl, R. Höhmann, J. Main, and H.-J. Stöckmann, Resonance Widths in Open Microwave Cavities Studied by Harmonic Inversion, Phys. Rev. Lett. **100**, 254101 (2008).
[44] J. Wiersig and J. Main, Fractal Weyl law for chaotic microcavities: Fresnel's laws imply multifractal scattering, Phys. Rev. E **77**, 036205 (2008).
[45] A. Di Falco, T.-F. Krauss, and A. Fratalocchi, Lifetime statistics of quantum chaos studied by a multiscale analysis, Appl. Phys. Lett. **100**, 184101 (2012).
[46] S. Barkhofen, T. Weich, A. Potzuweit, H.-J. Stöckmann, U. Kuhl, and M. Zworski, Experimental Observation of the Spectral Gap in Microwave N-Disk Systems, Phys. Rev. Lett. **110**, 164102 (2013).
[47] C. Liu, A. Di Falco, and A. Fratalocchi, Dicke Phase Transition with Multiple Superradiant States in Quantum Chaotic Resonators, Phys. Rev. X **4**, 021048 (2014).
[48] J.-B. Gros, U. Kuhl, O. Legrand, F. Mortessagne, E. Richalot, and D. V. Savin, Experimental Width Shift Distribution: A Test of Nonorthogonality for Local and Global Perturbations, Phys. Rev. Lett. **113**, 224101 (2014).
[49] L. Wang, D. Lippolis, Z.-Y. Li, X.-F. Jiang, Q. Gong, and Y.-F. Xiao, Statistics of chaotic resonances in an optical microcavity, Phys. Rev. E **93**, 040201(R) (2016).
[50] M. Davy and A. Z. Genack, Selectively exciting quasi-normal modes in open disordered systems, Nat. Commun. **9**, 4714 (2018).
[51] M. Davy and A. Z. Genack, Probing nonorthogonality of eigenfunctions and its impact on transport through open systems, Phys. Rev. Res. **1**, 033026 (2019).
[52] E. P. Wigner, Lower limit for the energy derivative of the scattering phase shift, Phys. Rev. **98**, 145 (1955).
[53] F. T. Smith, Lifetime matrix in collision theory, Phys. Rev. **118**, 349 (1960).
[54] E. Doron, U. Smilansky, and A. Frenkel, Experimental Demonstration of Chaotic Scattering of Microwaves, Phys. Rev. Lett. **65**, 3072 (1990).
[55] P. Ambichl, A. Brandstötter, J. Böhm, M. Kühmayer, U. Kuhl, and S. Rotter, Focusing inside Disordered Media with the Generalized Wigner-Smith Operator, Phys. Rev. Lett. **119**, 033903 (2017).

[56] Y. V. Fyodorov, Reflection time difference as a probe of s-matrix zeroes in chaotic resonance scattering, Acta Phys. Pol. A **136**, 785 (2019).
[57] N. Lehmann, D. Saher, V. V. Sokolov, and H.-J. Sommers, Chaotic scattering: The supersymmetry method for large number of channels, Nucl. Phys. A **582**, 223 (1995).
[58] N. Lehmann, D. V. Savin, V. V. Sokolov, and H.-J. Sommers, Time delay correlations in chaotic scattering: Random matrix approach, Physica D **86**, 572 (1995).
[59] Y. V. Fyodorov and H.-J. Sommers, Parametric Correlations of Scattering Phase Shifts and Fluctuations of Delay Times in Few-Channel Chaotic Scattering, Phys. Rev. Lett. **76**, 4709 (1996).
[60] Y. V. Fyodorov, D. V. Savin, and H.-J. Sommers, Parametric correlations of phase shifts and statistics of time delays in quantum chaotic scattering: Crossover between unitary and orthogonal symmetries, Phys. Rev. E **55**, R4857 (1997).
[61] P. W. Brouwer, K. M. Frahm, and C. W. Beenakker, Distribution of the quantum mechanical time-delay matrix for a chaotic cavity, Waves Random Media **9**, 91 (1999).
[62] D. V. Savin, Y. V. Fyodorov, and H.-J. Sommers, Reducing nonideal to ideal coupling in random matrix description of chaotic scattering: Application to the time-delay problem, Phys. Rev. E **63**, 035202 (2001).
[63] D. V. Savin and H. J. Sommers, Delay times and reflection in chaotic cavities with absorption, Phys. Rev. E **68**, 036211 (2003).
[64] A. Ossipov and Y. V. Fyodorov, Statistics of delay times in mesoscopic systems as a manifestation of eigenfunction fluctuations, Phys. Rev. B **71**, 125133 (2005).
[65] T. Kottos, Statistics of resonances and delay times in random media: Beyond random matrix theory, J. Phys. A **38**, 10761 (2005).
[66] F. Mezzadri and N. J. Simm, τ-function theory of quantum chaotic transport with $\beta = 1, 2, 4$, Commun. Math. Phys. **324**, 465 (2013).
[67] M. Novaes, Statistics of time delay and scattering correlation functions in chaotic systems. I. Random matrix theory, J. Math. Phys. **56**, 062110 (2015).
[68] F. D. Cunden, Statistical distribution of the Wigner-Smith time-delay matrix moments for chaotic cavities, Phys. Rev. E **91**, 060102 (2015).
[69] A. Grabsch, D. V. Savin, and C. Texier, Wigner-Smith time-delay matrix in chaotic cavities with non-ideal contacts, J. Phys. A **51**, 404001 (2018).
[70] A. Ossipov, Scattering Approach to Anderson Localization, Phys. Rev. Lett. **121**, 076601 (2018).
[71] A. Grabsch, Distribution of the Wigner-Smith time-delay matrix for chaotic cavities with absorption and coupled Coulomb gases, J. Phys. A **53**, 025202 (2020).
[72] A. Grabsch and C. Texier, Wigner-Smith matrix, exponential functional of the matrix Brownian motion and matrix Dufresne identity, arXiv:2002.12077.
[73] C. Texier, Wigner time delay and related concepts: Application to transport in coherent conductors, Physica E **82**, 16 (2016).
[74] Y. V. Fyodorov, M. Titov, and H. J. Sommers, Statistics of S-matrix poles for chaotic systems with broken time reversal invariance: A conjecture, Phys. Rev. E **58**, R1195 (1998).
[75] J. J. M. Verbaarschot, H. A. Weidenmüller, and M. R. Zirnbauer, Grassmann integration in stochastic quantum physics: The case of compound-nucleus scattering, Phys. Rep. **129**, 367 (1985).
[76] P. Vidal and E. Kanzieper, Statistics of Reflection Eigenvalues in Chaotic Cavities with Nonideal Leads, Phys. Rev. Lett. **108**, 206806 (2012).
[77] A. M. Martínez-Argüello, R. A. Méndez-Sánchez, and M. Martínez-Mares, Wave systems with direct processes and localized losses or gains: The nonunitary Poisson kernel, Phys. Rev. E **86**, 016207 (2012).
[78] M. Lawniczak and L. Sirko, Investigation of the diagonal elements of the Wigner's reaction matrix for networks with violated time reversal invariance, Sci. Rep. **9**, 5630 (2019).
[79] P. Gaspard, and S. A. Rice, Scattering from a classically chaotic repellor, J. Chem. Phys. **90**, 2225 (1989).
[80] P. Gaspard and S. A. Rice, Semiclassical quantization of the scattering from a classically chaotic repellor, J. Chem. Phys. **90**, 2242 (1989).
[81] Y. V. Fyodorov, H.-J. Sommers, and B. Khoruzhenko, Universality in the random matrix spectra in the regime of weak non-Hermiticity, Ann. Inst. H. Poincaré Phys. Théor. **68**, 449 (1998).